J Mol Model (2012) 18:3455–3466
DOI 10.1007/s00894-011-1336-5

ORIGINAL PAPER

A test of improved force field parameters for urea: molecular-dynamics simulations of urea crystals

Gül Altınbaş Özpınar · Frank R. Beierlein · Wolfgang Peukert · Dirk Zahn · Timothy Clark

Received: 16 November 2011 / Accepted: 5 December 2011 / Published online: 27 January 2012

Abstract Molecular-dynamics (MD) simulations of urea crystals of different shapes (cubic, rectangular prismatic, and sheet) have been performed using our previously published force field for urea. This force field has been validated by calculating values for the cohesive energy, sublimation temperature, and melting point from the MD data. The cohesive energies computed from simulations of cubic and rectangular prismatic urea crystals *in vacuo* at 300 K agreed very well with the experimental sublimation enthalpies reported at 298 K. We also found very good agreement between the melting points as observed experimentally and from simulations. Annealing the crystals just below the melting point leads to reconstruction to form crystal faces that are consistent with experimental observations. The simulations reveal a melting mechanism that involves surface (corner/edge) melting well below the melting point, and rotational disordering of the urea molecules in the corner/edge regions of the crystal, which then facilitates the translational motion of these molecules.

Keywords Crystal simulations · Force field · Molecular dynamics · Urea

Gül Altınbaş Özpınar and Frank R. Beierlein contributed equally to this work

Electronic supplementary material The online version of this article (doi:10.1007/s00894-011-1336-5) contains supplementary material, which is available to authorized users.

G. A. Özpınar
Department of Chemistry, Natural Sciences,
Architecture and Engineering Faculty, Bursa Technical University,
Osmangazi 16000 Bursa, Turkey

G. A. Özpınar · F. R. Beierlein · D. Zahn · T. Clark
Computer-Chemie-Centrum and Interdisciplinary
Center for Molecular Materials,
Friedrich-Alexander Universität Erlangen-Nürnberg,
Nägelsbachstr. 25,
91052 Erlangen, Germany

G. A. Özpınar · F. R. Beierlein · W. Peukert · D. Zahn · T. Clark (✉)
Excellence Cluster Engineering of Advanced Materials,
Friedrich-Alexander-Universität Erlangen-Nürnberg,
Nägelsbachstr. 49b,
91052 Erlangen, Germany
e-mail: Tim.Clark@chemie.uni-erlangen.de

W. Peukert
Lehrstuhl für Feststoff- und Grenzflächenverfahrenstechnik,
Friedrich-Alexander-Universität Erlangen-Nürnberg,
Cauerstraße 4,
91058 Erlangen, Germany

Introduction

In principle, classical mechanics (force field) simulations can be used to investigate crystal morphologies and forms. However, deriving appropriate parameters for a simple, non-polarizable force field able to reproduce crystal structures and properties is not trivial. In the following, we report a validation study on a force field previously derived purely from *ab initio* calculations on simple molecular aggregates in order to determine how well force-field parameters for crystal studies can be derived *ab initio*.

Urea is a common component of many products and has been used for a wide range of purposes, e.g., as a powerful protein denaturant, a stabilizer in nitrocellulose explosives, a cloud-seeding agent, for flame-proofing, and as a nitrogen source [1]. Urea crystals possess interesting nonlinear optical properties [2] and urea can form clathrates [3] and act as a ligand in transition-metal complexes [4]. It has been investigated intensively, both theoretically and experimentally, since it represents a prototypical small molecule that interacts strongly with environments such as solvent, organic guest

molecules and biomolecular systems. Since intermolecular interactions in condensed phases perturb the electronic structures of the urea molecule from its gas-phase optimum significantly, it is crucial to use appropriate force-field potentials when simulating solids or solutions. Many molecular-dynamics (MD) simulations of urea interactions with water and organic compounds have been reported. Boek et al. [5, 6] simulated urea–water systems using general purpose biomolecular force fields and analyzed these in terms of the total nitrogen scattering function ($G_N(r)$) by comparing their results with neutron scattering data. However, they concluded that reproducing $G_N(r)$ does not constitute a very stringent test of the force-field potentials. Åstrand et al. [7, 8] constructed non-emprical modeling (NEMO) potentials for the urea–water system and analyzed the radial distribution functions obtained from MD simulations. They investigated the urea dimerization energy because the formation of urea dimers and larger oligomers plays an important role in urea nucleation, aggregation and behavior in aqueous solution. Nevertheless, their computed data differed from those of Boek et al. [5] and Cristinziao et al. [9] in which the GROMOS force field [10] combined with the HHL (Hagler – Huler – Lifson) parameters [11] for intermolecular interactions was used. These differences can be traced back entirely to the different force fields used, [12, 13] underlining the importance of an accurate and consistent set of parameters for urea.

In our previous study, [14] we described a refined force field based on the generalized AMBER force field [15] (GAFF) for urea. We investigated energies and geometrical parameters of seven different urea dimer structures, which were optimized at the MP2/aug-cc-pVDZ level [16, 17] to obtain accurate interaction energies. Atomic partial charges were calculated at the MP2/aug-cc-pVDZ level with the restrained electrostatic potential (RESP) [18] fitting approach. In order to fit urea-urea interactions obtained from high level *ab initio* calculations, the interaction energies were computed with these new RESP charges in the force field and the results were consistent with those obtained from CCSD and MP2 calculations. The linear dimer structure optimized using the force field with modified geometrical parameters and the new RESP charge set agreed well with the experimental urea crystal data [19–21]. In this work, we validate this force field for molecular-dynamics simulations of crystalline urea systems. For this purpose, we used the three different urea crystal morphologies shown in Fig. 1 (cubic, rectangular prismatic, and sheet) and analyzed data obtained from the simulations of these urea crystal models. Simulated values for cohesive energy, sublimation temperature, and melting point are compared to the available experimental and theoretical data. Moreover, the molecular mechanism of melting in these nanocrystals is investigated in detail.

Methods

Urea crystal models and force field

Urea crystal systems in cubic, rectangular prismatic, and sheet geometries, containing 1152, 1125, and 1220 urea molecules, respectively, (Fig. 1) were constructed by replication of the unit cell (8×8×8, 20×5×5, and 20×1×20) in the a, b, and c directions, respectively, using Materials Studio 5.0 [22]. The force field parameters and RESP charge set used in the MD simulations are those reported earlier [14] and are shown once more in Tables S1 and S2 of the Supplementary material.

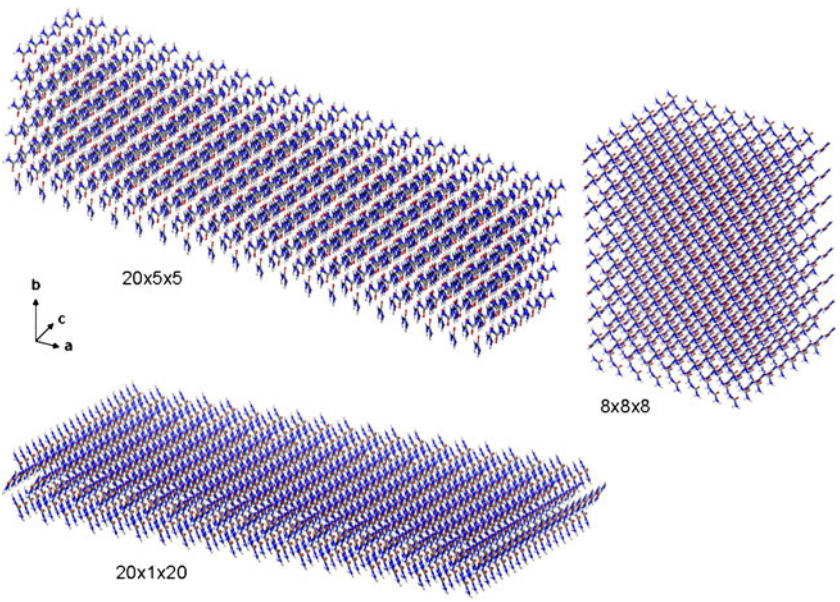

Fig. 1 The urea crystal models studied. They consist of 1152, 1125, and 1220 urea molecules in cubic (8×8×8), rectangular prismatic (20×5×5), and sheet (20×1×20) shapes, respectively

MD simulation setup and protocol – initial crystal simulations *in vacuo*

All MD simulations were carried out using the AMBER 10 biomolecular simulation package [23]. All interactions were treated using the refined GAFF parameter set described previously [14]. Initially, the urea crystals constructed as explained above were minimized using 100,000 steps of steepest-descent minimization. The structures thus obtained served as inputs for initial Langevin-dynamics simulations of the cubic, rectangular prismatic, and sheet urea crystal models *in vacuo* at 300 K using a collision frequency of 1 ps^{-1}. Non-bonded interactions (electrostatic and Lennard-Jones) were treated using a cutoff of 12 Å, periodic boundary conditions were not used in this case. An integration time step of 1.0 fs was chosen, and quantities such as energy and atomic coordinates were stored every ps. These initial simulations were run *in vacuo* for 10 ns.

Simulation protocol for heating the cubic urea crystal model

In a second series of simulations, the cubic crystal system consisting of 1152 urea molecules (crystal dimensions approximately 45×45×35 Å) was enclosed in a larger periodic box (approximately 250×250×240 Å) to allow urea sublimation from the nanoparticle in the course of heating. After initial minimization (10,000 steps of steepest-descent minimization), constant-volume (NVT) periodic boundary MD simulations were performed using an integration time step of 1 fs. In this second set of simulations, the Particle Mesh Ewald [24, 25] method was used to treat electrostatic interactions and a cutoff of 12 Å was used for the van-der-Waals interactions. Langevin-dynamics temperature control was used with a collision frequency of 2.0 ps^{-1}. Energies and coordinates were stored every ps. Initial system heat-up (see below) was performed rapidly in the first picoseconds of a first 500 ps partial trajectory, in which weak restraints (10 kcal mol^{-1} $Å^{-2}$) were applied on all urea atoms, all further simulation steps were unrestrained.

We used two different simulation schemes to heat up the cubic crystal structure: "instantaneous" and "gradual heating". In the first one, we simulated the system at a series of temperatures (300, 350, 370, 380, 382, 385, 390, 400, 450, 500, and 550 K), after initial heat-up to the target temperature (see above) during the first (approximately) 5 ps. Simulations were run for 61 ns at 380 and 382 K, 36 ns at 550 K and 11 ns at the other temperatures. In the "gradual heating" simulations, the system was initially equilibrated as described above for 3 ns at 273 K. In the further simulation steps, the system was gradually heated up to 453 K (in one case, 20 K ns^{-1}, to 553 K) using four different heating rates: 5, 10, 20 and 30 K ns^{-1}, i.e., the final temperature was reached after 39, 21, 17 and 9 ns of total simulation time.

Cohesive energies

Cohesive energies of the cubic, rectangular prismatic, and sheet crystal systems were calculated using Eq. 1 [26, 27]:

$$\Delta E = \frac{E_{bulk}}{Z} - E_{mol}, \quad (1)$$

where E_{bulk} is the total energy of bulk (i.e., the whole simulation system), Z is the number of molecules in the bulk, and E_{mol} is the total energy of one isolated molecule simulated in the gas phase (at the corresponding temperature). Cohesive energies were calculated for the three crystal morphologies

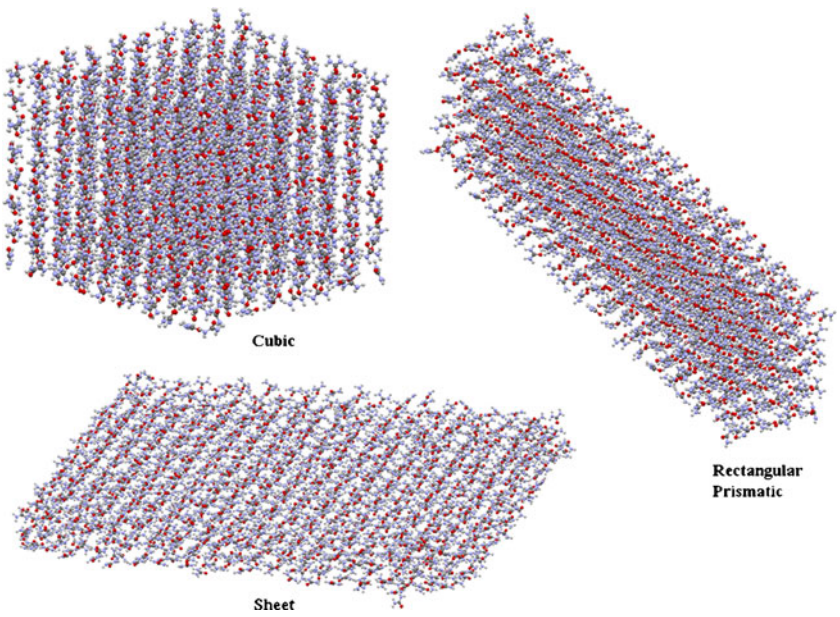

Fig. 2 The urea crystal structures after non-periodic simulations in vacuo at 300 K for 10 ns

Table 1 Comparison of calculated and experimental values (kcal mol^{-1}) for cohesive energies of urea

This work				Quantum chemical calculations		
Z^a	**Method**	**T**	**ΔE**	Z^a	**Method**	**ΔE**
1125	MD simulation (rectangular prismatic)	300 K	−20.87	2	HF/6-31G(d,p)	−14.72[g]
1152	MD simulation (cubic)	300 K	−22.82	2	SVWN/6-31G(d,p)	−33.13[g]
1220	MD simulation (sheet)	300 K	−11.25	2	PW91/6-31G(d,p)	−18.95[g]
				2	PBE/6-31G(d,p)	−17.85[g]
Experimental				2	PBE(0)/ 6-31G(d,p)	−18.57[g]
Technique		**T**	**ΔE**	2	B3LYP/6-31G(d,p)	−15.80[g]
Knudsen		298K	−20.95[b]	2	B3LYP/DZP	−16.01[g]
Torsion		298K	−22.53[c]	2	B3LYP/6-311G(d,p)	−15.63[g]
Transpiration		298K	−22.82[d]	2	B3LYP/TZP	−16.25[g]
Knudsen		298K	−22.93[e]	2	B3LYP–D*/6-31G(d,p)	−24.92[h]
Torsion-Knudsen		298K	−23.56[f]	2	B3LYP–D*/TZP	−25.52[h]
				6	MP2/6-31G(d)	−52.70[i]
				10	MP2/6-31G(d)	−58.50[i]
				6	HF/6-31G(d)	−52.20[i]
				10	HF/6-31G(d)	−53.30[i]
				14	HF/6-31G(d)	−47.30[i]
				18	HF/6-31G(d)	−45.30[i]
				22	HF/6-31G(d)	−39.80[i]
				11	MP2+DFT	−21.50[j]
				17	MP2+DFT	−21.30[j]
				37	MP2+DFT	−21.50[j]
				55	MP2+DFT	−21.80[j]
				65	MP2+DFT	−21.90[j]
				93	MP2+DFT	−22.20[j]
				129	MP2+DFT	−22.40[j]

[a] Number of urea molecules
[b] Taken from [30]
[c] Taken from [31]
[d] Taken from [32]
[e] Taken from [33]
[f] Taken from [34]
[g] Taken from [26]
[h] Taken from [27]
[i] Taken from [35]
[j] Taken from [36]

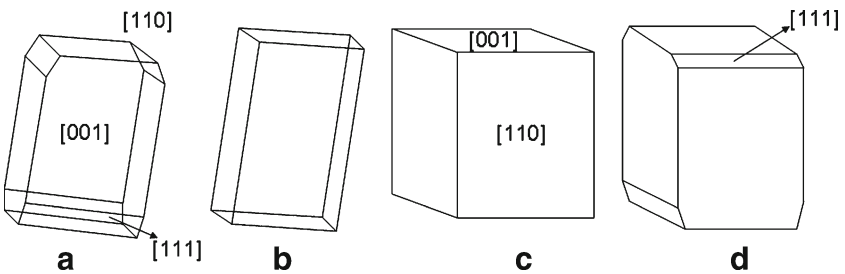

Fig. 3 The morphology of vapor-grown urea crystals determined experimentally (**a**) and theoretically using distributed multipole analysis (DMA) force fields (**b**), (adapted from Ref [37]), growth form according to attachment energy and Ising models (**c**), and equilibrium form (**d**), adapted from Ref [38]

investigated ("cubic", "rectangular prismatic" and "sheet") using simulation data from the non-periodic simulations of the crystals *in vacuo* at 300 K.

Root mean square fluctuations and mean interaction energies – initial crystal simulations *in vacuo*

To investigate the mobility and interaction energies of the urea molecules with the remainder of the system, the trajectories obtained from the non-periodic simulations of the cubic, rectangular prismatic and sheet crystals *in vacuo* at 300 K were overlaid on their first frame using the urea heavy atoms as fitting mask, and the root mean square fluctuations (RMSFs) and average coordinates (for the heavy atoms of each urea molecule) were calculated using the Amber 10 ptraj tool [23]. Mean interaction energies (van der Waals, electrostatic and total) between all individual residues and the rest of the system were calculated using the Amber 9 anal tool [28]. These values were mapped on the geometric centers of the average coordinates of the heavy atoms in each urea molecule. The analyses of interaction energies were performed using the non-periodic simulation data as the Amber tool anal does not support periodic boundary conditions.

Root mean square fluctuations and orientational order parameters

To investigate the melting process in detail, a selection of the MD trajectories obtained from the periodic-boundary simulations explained above ("instantaneous heating": 300 K, 350 K and 382 K; "gradual heating": 5 K ns^{-1}) was overlaid on the initial structure (before minimization) using all urea carbon atoms as fitting mask (the Amber 10 ptraj tool [23] was used for fitting and RMSD/RMSF calculation). The corresponding system root-mean-square deviation (RMSD) and the molecule root-mean-square fluctuations (RMSFs) were obtained and analyzed as a measure of translational motion in the system. The initial 500 ps (restrained MD, heat-up) were omitted in these and the following analyses. To obtain information about rotational motion/disorder in the heating/melting process, we also calculated orientational order parameters for each molecule [29]:

$$S_{mol} = \frac{(3\langle \cos^2 \varphi \rangle - 1)}{2} \quad (2)$$

$$\cos \varphi = \vec{n} \bullet \vec{u}. \quad (3)$$

Brackets denote the ensemble average of $\cos^2\varphi$ over the simulation snapshots, **n** is the unit vector in the direction of the *c*-axis of the initial conformation and **u** is the unit vector in the direction of the C=O axis in the individual urea molecules. The orientational order parameter for the whole system was obtained as the mean of the values for individual molecules (N: number of molecules):

$$S_{sys} = \frac{1}{N} \sum^{N} \frac{(3\langle \cos^2 \varphi \rangle - 1)}{2}. \quad (4)$$

The RMSF values and the molecular order parameters thus obtained were visualized by mapping them onto the initial coordinates of the C atoms of all urea molecules in the cubic crystal.

Table 2 Experimental sublimation temperatures for urea

T_{sub} (K)	Ref.
354	[39]
345-368	[40], [30]
338-362	[34]
361	[41]
357	[42]
381	[43]

Results and discussion

Cohesive energies

The three different urea crystal structures simulated are shown in Fig. 2. The variations of RMSD, RMSF, interaction energy, total energy, and temperature during the initial crystal simulations *in vacuo* are shown in the Supporting information. The cohesive energies of these structures computed from the simulations *in vacuo* at 300 K are compared with the experimental sublimation enthalpy [30–34] and the

Table 3 "Instantaneous heating" protocol

T [K]	t [ns]	Comment
300	11	Crystal, corners truncated ([111]+images), rearrangement+mobile layer on [001]
350	11	as above, additionally edges ([110]) begin to be truncated
370	11	as above, additionally edges ([110]) begin to be truncated
380	61	Crystal, corners ([111])+edges ([110]) truncated, rearrangement+mobile layer on [001]
382	61	as above
385	11	Fluid droplet
390	11	Fluid droplet
400	11	Fluid droplet
450	11	Fluid droplet, 2 urea in gas phase
500	11	Fluid droplet, ~ 5 in the gas phase
550	36	Fluid droplet, ~ 29 in the gas phase

reported theoretical cohesive [26, 27] and lattice [35–37] energies in Table 1. The energies for cubic and rectangular prismatic urea systems agree well with the experimental values, whereas that of the sheet structure is significantly less negative. This is in accord with the fact that the cubic and rectangular prismatic urea crystal structures bear a close resemblance to both the experimental (vapor grown) [37] and theoretical [38] morphological structures (Fig. 3).

The highest cohesive energy calculated (that for the cubic crystal, -22.8 kcal mol^{-1}) lies in the center of the range given by experiment, [30–34] suggesting that the intermolecular (van der Waals, Coulomb) components of the force field [14] are appropriate for condensed phases.

As expected, the MD simulations of cubic and rectangular prismatic urea crystals performed better than the quantum chemical computations reported by Civalleri et al. [26, 27] and Gora et al. [35]. The SVWN method overestimated the experimental data by approximately 10 – 13 kcal mol^{-1} and the other levels underestimated it by about 5 – 8 kcal mol^{-1}. These results illustrate the problems with basis-set superposition

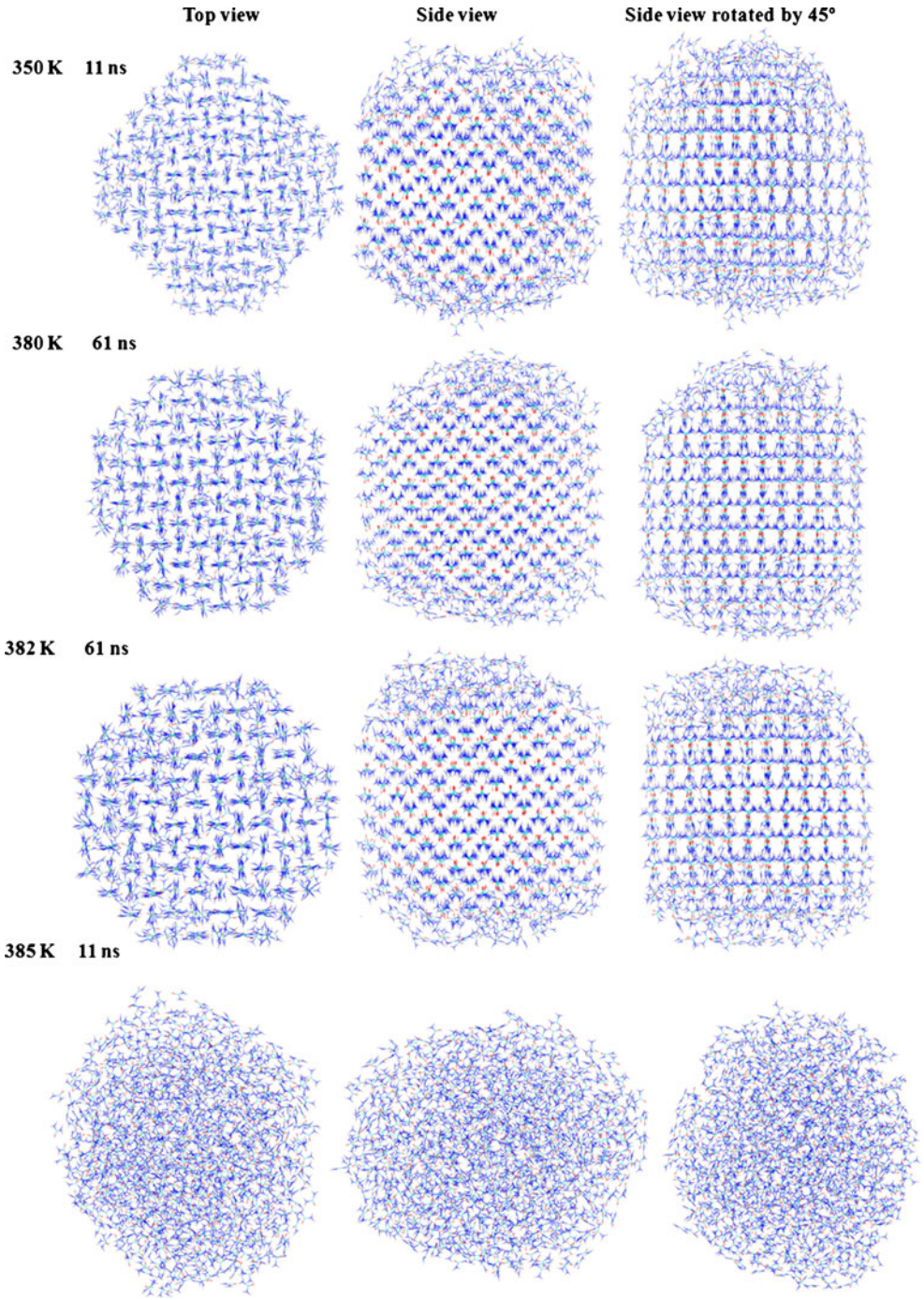

Fig. 4 Snapshots from the MD simulations at 350, 380, 382, and 385 K using the "instantaneous heating" protocol

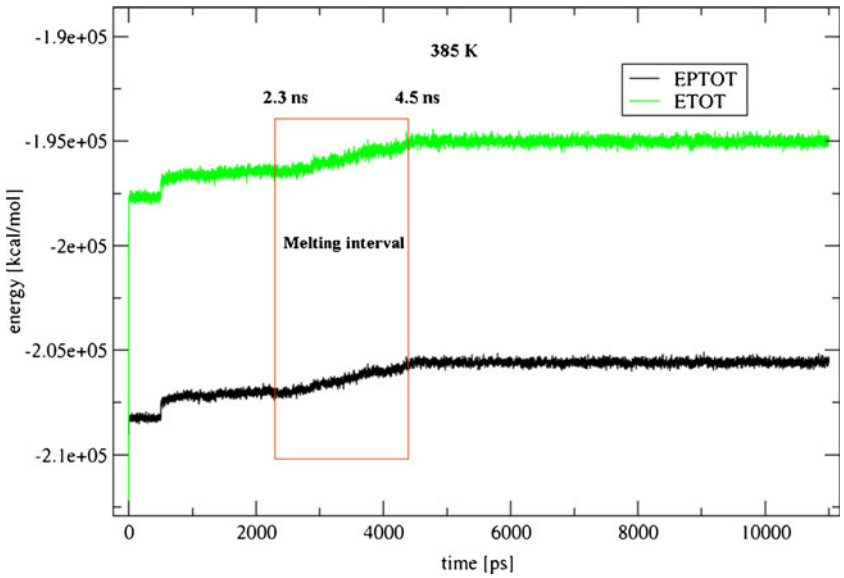

Fig. 5 Total (green) and potential energies (black) obtained from the "instantaneous heating" protocol MD simulation at 385 K

error (BSSE), which causes oligomerization energies to be too high, and the inability of Hartree-Fock and DFT techniques to reproduce dispersion, which gives the opposite trend. Adding a classical two-center dispersion term (as used by the force fields) to DFT gives better results, [27] but the calculated oligomerization energies are still 2.0 – 4.6 kcal mol^{-1} higher than the experimental values. Gora et al. [35] studied models for the molecular crystal urea containing 6 – 22 urea molecules and compared the calculated total interaction energies with the experimental data but used the 6-31G(d) basis set, which gives a large BSSE. They also concluded that increasing the cluster size reduced the magnitude of interaction energy per molecule, so that a further extension of the cluster size would probably lead to better agreement with the experiment, which is also consistent with a large BSSE. Tsuzuki et al. [36] proposed a method for computing lattice energies of urea clusters (11 – 129 urea molecules) using a combination of a periodic DFT calculation and MP2 calculations of two-body interactions with neighboring molecules. The electrostatic interactions and the interactions with neighboring molecules (for the dispersion contributions) were evaluated by a periodic DFT calculation and the MP2 calculations, respectively. Their results agree well with the experimental data.

Sublimation temperature and melting point

The sublimation temperatures of urea determined experimentally using different techniques [30, 34, 39–43] are shown in Table 2. The melting point of urea is reported to be 405.9 K [44]. The MD simulations performed using the "instantaneous heating" protocol (see above, Sect. 2.3) are summarized in Table 3.

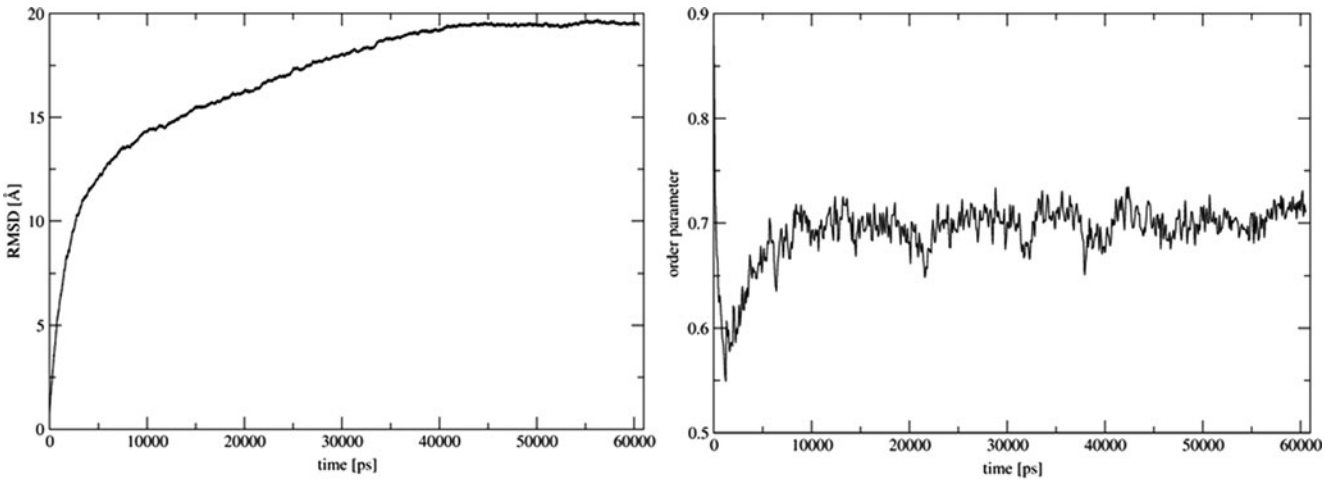

Fig. 6 RMSD (left) and orientational order parameter (right) calculated for all carbon atoms obtained from the "instantaneous heating" protocol MD simulation at 382 K. The first 500 ps (restrained MD, heat-up) were omitted for the analyses

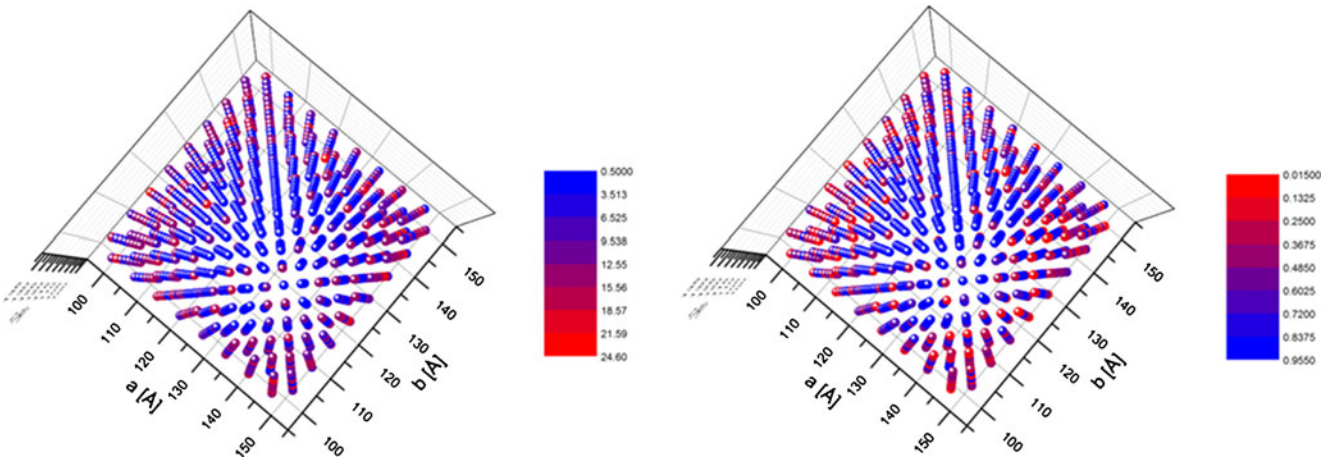

Fig. 7 RMSF (left) and orientational order parameter (right) calculated for all carbon atoms mapped on the initial coordinates of all C atoms in the system, as obtained from the "instantaneous heating" protocol MD simulation at 382 K. The viewing angle corresponds to "top view" in Fig. 4. The first 500 ps (restrained MD, heat-up) were omitted for the analyses

Table 3 and Fig. 4 show that a truncation of the corners ([111] faces and their symmetry images) and a high mobility of urea molecules on the [001] surfaces of the cubic urea crystal are visible at 300 K and pronounced at 350 K. Experimental estimates of the sublimation temperature lie between 345 and 381 K, so that we would not only expect to observe the onset of mobility for individual molecules at 350 K, but also sublimation. However, in our simulations above sublimation temperature only very few urea molecules leave the aggregate (at 450 K, 500 K and 550 K, see Table 3), because of the limited time scales accessible in MD. Our observation that the urea nanocrystal melts from the corners, edges and surfaces is in good agreement with the experimentally observed "surface melting" phenomenon, which is observed for surfaces in many systems, also molecular crystals [45]. Interestingly, the face with the highest mobility is the [001] surface, which is also one of the dominating surfaces of vapor-grown urea crystals [37]. This indicates a low interaction energy of the molecules on this face with the crystal lattice. This is consistent with the "attachment energy method" for predicting crystal morphologies, [37] which proposes that crystal faces with low attachment energy remain in the crystal growth process and thus dominate the gas-phase-grown crystal habitus, while faces with high attachment energies "grow out" and vanish. Surface melting in the urea nanocrystal simulated here can be attributed to the weaker interaction and therefore higher mobility of the urea molecules in the corners, edges and surfaces compared to the bulk. An illustration of the weakening of interaction energies of the urea molecules at these surface positions is shown in the Supporting information (Fig. S2), calculated from the vacuum simulation data explained above. Fig. S2 also shows the weaker interaction of the [001] surface with the remainder of the system.

Analysis of the trajectories shows that the crystal lattice still exists in the center of the urea cluster at 380 and 382 K, even after 61 ns (Fig. 4). However, the crystal melts completely at 385 K. Potential and total energy graphs shown in Fig. 5 also verify that the urea crystal begins to melt at 385 K after 2.30 ns and is completely molten after 4.55 ns. The melting point thus obtained from our "instantaneous heating" MD protocol (between 382 and 385 K) is approximately 20 K lower than the experimental value (405.9 K) [44]. Interestingly, it is frequently observed that small clusters melt well below the bulk melting temperature. Thus, the melting point discrepancy

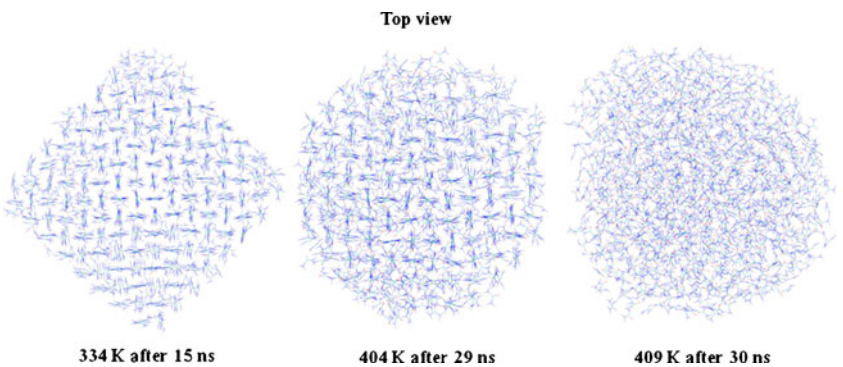

Fig. 8 Snapshots from the MD simulation using the "gradual heating" protocol and a heating rate of 5 K ns^{-1}

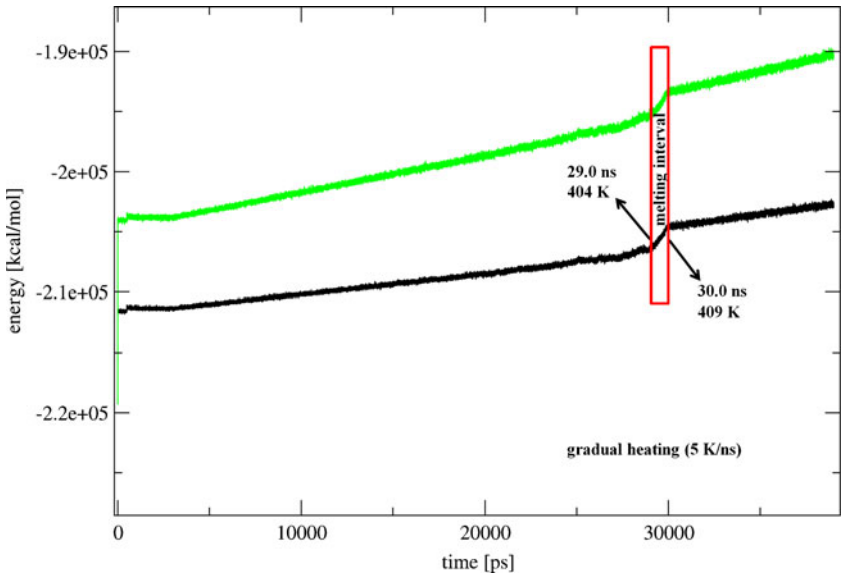

Fig. 9 Plots of total (green) and potential energies (black) obtained from the MD simulation using the "gradual heating" protocol and a heating rate of 5 K ns^{-1}

observed here could, at least in part, be attributed to such a size effect [45]. However, as methodical errors could also account for this discrepancy, the melting point is also assessed using the alternative "gradual heating" MD simulations, as discussed below.

In order to investigate the melting mechanism in more detail, especially whether molecular translation or rotation ("rotational melting") dominates first, we analyzed the evolution of system root-mean-square deviation (RMSD), calculated for all carbon atoms, and the orientational order parameter (which describes the deflection of the C=O axis of the urea molecules from the crystallographic c-axis) vs. time (Fig. 6 and Supporting information Figs. S6 and S7) at different temperatures (300 K, 350 K and 382 K). In the 300 K simulation (Fig. S6), the system RMSD increases to about 3.9 Å after 11 ns, and the system order parameter decreases to about 0.73 after 11 ns. In the simulation at 350 K (Fig. S7), an increased system RMSD is observed (~8.6 Å after 11 ns), and the system order parameter drops much quicker to values of approximately 0.68, and reaches a final value of 0.70 after 11 ns. In the simulation just below the (computational) melting point (382 K, Fig. 6), the system RMSD increases quickly and reaches a plateau with values of about 19.5 Å after about 42 ns (19.46 Å after 61 ns). At this temperature, the orientational order parameter decreases rapidly to a value of 0.55 after 1.7 ns, rises again and reaches a plateau of about 0.7 after about 8.7 ns (final value 0.71 after 61 ns). Generally, the RMSD increases and the order parameter decreases with increasing temperature with the exception that at 382 K (just below the melting point) we observe an increase in the order parameter value after an initial minimum.

In order to investigate differences between the crystal surfaces, we mapped molecular root-mean-square fluctuations (RMSFs) and molecular order parameters onto the coordinates of the central carbon atom of the urea molecules at their initial positions (Fig. 7 and Supporting information Figs. S8 and S9). These plots revealed no significant differences between the faces of the original cubic crystal, so that no preference of rotation/translation of molecules at the [100], [001] and [010] surfaces can be identified. The truncation of the (artificial) crystal along the emerging [110] and [111] surfaces, however, is clearly visible from these plots.

In a second attempt to determine the melting point of urea as represented by our parameterization, we performed four molecular-dynamics simulations using our "gradual heating" protocol (gradual heating from 273 K) and four different heating rates (30, 20, 10 and 5 K ns^{-1}, see Sect. 2.3 for more details, and Figs. S10-S13 in the Supporting information). After the cubic urea crystal system was equilibrated at 273

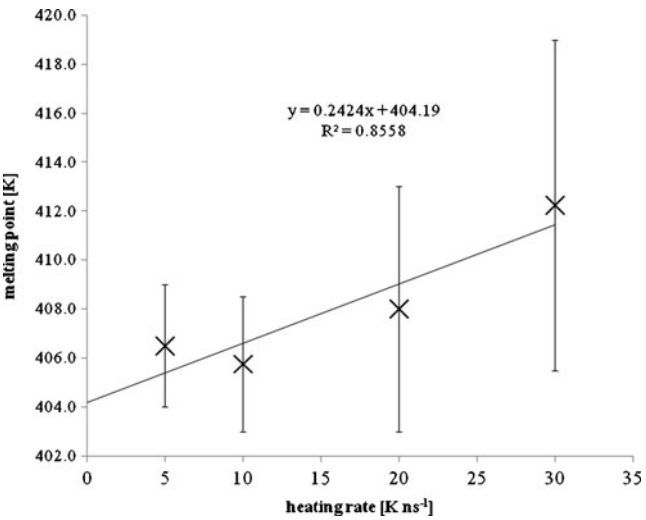

Fig. 10 Plot of melting point (mean value of melting interval boundaries) obtained from the MD simulations using the "gradual heating" protocol and different heating rates. Error bars represent the lower and upper boundaries of the melting interval

K for 3 ns, the temperature was increased by 30, 20, 10 and 5 K ns^{-1}, respectively, until the final temperature of 453 K (553 K in the case of the 20 K ns^{-1} simulation) was reached (after 9, 17, 21 and 39 ns, respectively). Snapshots and plots of the total and potential energies of the system from the simulation using a heating rate of 5 K ns^{-1} are shown in Figs. 8 and 9, the corresponding energy plots for the other heating rates investigated (30, 20 and 10 K ns^{-1}) are shown in the Supporting information (Figs. S14-S16). In all four simulations (30, 20, 10 and 5 K ns^{-1}, crystal reorganization and surface melting start below the experimental sublimation temperature (354 K); they are clearly visible at approximately 334 K. Melting of the crystalline core can be determined easily from the potential-energy curves (Figs. 9, S14-S16). The step in the potential-energy curve clearly shows the beginning and end of the phase transition of the crystalline core, in perfect agreement with visual inspection. This step is preceded by a kink in the potential-energy curve, which occurs at 396, 384, 395, and 392 K (5, 10, 20 and 30 K ns^{-1} simulations, respectively) and indicates increased surface melting. In the 5 K ns^{-1} simulation, which should be the closest to the experimental situation, the core regions of the cubic crystal melt between 404 and 409 K (mean: 406.5 K, 29.0 - 30.0 ns), in the 10 K ns^{-1} simulation a melting interval of 403 - 408.5 K (15.9-16.45 ns, mean value 405.75 K ns^{-1}) is determined, and in the 20 K ns^{-1} simulation core melting starts at 403 K (9.5 ns), and the crystal is completely molten at 413 K (10.0 ns, mean value 408 K). In the simulation with the fastest heating rate (30 K ns^{-1}), core melting begins at 405.5 K (7.4 ns) and the crystal is completely molten at 419 K (7.85 ns, mean value 412.25 K). For the 5 K ns^{-1} simulation, RMSD and order parameter are plotted vs. time in Supporting information Fig. S18; they, too, allow the determination of the melting process.

Extrapolating the mean values of the upper and lower melting interval boundaries to a heating rate of 0 K ns^{-1} gives a corrected melting point of 404.2 K (R^2=0.86, Fig. 10), which is in surprisingly good agreement with the experimental value of 405.9 K [44]. Thus, the comparison of the two approaches shows the gradual heating approach to be more appropriate than "brute-force" instantaneous heating, even when applying tethering forces to avoid instantaneous melting.

Conclusions

The validation simulations reported above suggest that the modified GAFF force field for urea reported earlier [14] performs well reproducing experimental data available for urea crystals. This is an important conclusion because the force field was parameterized exclusively based on *ab initio* calculations of different conformations of the urea dimer. Thus, calculating relatively small molecular aggregates at sufficiently high levels of *ab initio* theory provides a force field that can reproduce crystal properties surprisingly well. This is significant because the GAFF force field used in this work is extremely simple and represents essentially the minimum complexity for an atomistic force field intended to reproduce complex intermolecular interactions. The strategy employed to develop the force field implies that intermolecular polarization is implicit in its Coulomb potentials, as has often been proposed, for instance protein or force fields [46]. This implicit polarization moves the physical model represented by the force field away from the real situation, so that the good performance of the crystal simulations is both surprising and encouraging.

There are clearly cases (above all, for water) in which implicit polarization will be a far less satisfactory approximation than for urea crystals. However, given the importance of organic crystal morphology, [47, 48] the possibility of a multi-scale approach in which the force field can be parameterized to reproduce *ab initio* results for dimers and other small aggregates before simulations are used to investigate crystals or nucleation [49–52] represents an important step forward. We note that the systematic improvability of *ab initio* calculations is important in this respect. It is possible that parameterized DFT methods may also be useful, but they do not allow the results for intermolecular interactions to be tested systematically and the force field to be based on a level that reproduces the converged results.

Acknowledgments This work was supported by the Deutsche Forschungsgemeinschaft as part of the project PE 42710-2 and the Excellence Cluster *Engineering of Advanced Materials.*

References

1. Bonin M, Marshall WG, Weber HP, Tolendo P (1999) Polymorphism in urea. IOP Publishing ISIS. http://www.isis.rl.ac.uk/archive/isis99/highlights/urea4.htm. Accessed August 1999.
2. Mathews CK, van Holde KE (1996) Biochemistry, 2nd edn. Cummings, Menlo Park, CA, p 4
3. Bhatnagar VM (1968) Clathrates of urea and thiourea. J Struct Chem 8:513–529. doi:10.1007/BF00751656
4. Theophanides T, Harvey PD (1987) Structural and spectroscopic properties of metal-urea complexes. Coord Chem Rev 76:237–264. doi:10.1016/0010-8545(87)85005-1
5. Boek ES, Briels WJ (1993) Molecular dynamics simulations of aqueous urea solutions: Study of dimer stability and solution structure, and calculation of the total nitrogen radial distribution function GN(r). J Chem Phys 98:1422–1427. doi:10.1063/1.464306
6. Boek ES, Briels WJ, van Eerden J, Feil D (1992) Molecular-dynamics simulations of interfaces between water and crystalline urea. J Chem Phys 96:7010–7018. doi:10.1063/1.462560
7. Åstrand PO, Wallqvist A, Karlström G (1994) Molecular dynamics simulations of 2M aqueous urea solutions. J Phys Chem 98:8224–8233. doi:10.1021/j100084a046
8. Åstrand PO, Wallqvist A, Karlström G (1994) Nonempirical intermolecular potentials for urea – water systems. J Chem Phys 100:1262–1273. doi:10.1063/1.466655

9. Cristinziao P, Lelj F, Amodeo P, Barone V (1987) A molecular dynamics study of associations in solution. An NPT simulation of the urea dimer in water. Chem Phys Lett 140:401–405. doi:10.1016/0009-2614(87)80755-8
10. Hermans J, Berendsen HJC, van Gunsteren WF, Postma JPM (1984) A consistent empirical potential for water–protein interactions. Biopolymers 23:1513–1518. doi:10.1002/bip.360230807
11. Hagler AT, Huler E, Lifson S (1976) Energy functions for peptides and proteins. I. Derivation of a consistent force field including the hydrogen bond from amide crystals. J Am Chem Soc 96:5319–5327. doi:10.1021/ja00824a004
12. Kallies B (2002) Coupling of solvent and solute dynamics—molecular dynamics simulations of aqueous urea solutions with different intramolecular potentials. Phys Chem Chem Phys 4:86–95. doi:10.1039/b105836n
13. Caballo-Herrera A, Nilsson L (2006) Urea parameterization for molecular dynamics simulations. J Mol Struct THEOCHEM 758:139–148. doi:10.1016/j.theochem.2005.10.018
14. Özpınar GA, Peukert W, Clark T (2010) An improved generalized AMBER force field (GAFF) for urea. J Mol Mod 16:1427–1440. doi:10.1007/s00894-010-0650-7
15. Wang J, Wolf RM, Caldwell JW, Kollman PA, Case DA (2004) Development and testing of a general amber force field. J Comput Chem 25:1157–1174. doi:10.1002/jcc.20035
16. Moller C, Plesset MS (1934) Note on an Approximation Treatment for Many-Electron Systems. Phys Rev 46:618–622. doi:10.1103/PhysRev.46.618
17. Dunning TH Jr (1989) Gaussian basis sets for use in correlated molecular calculations. I. The atoms boron through neon and hydrogen. J Chem Phys 90:1007–1023. doi:10.1063/1.456153
18. Bayly CI, Cieplak P, Cornell WD, Kollman PA (1993) A well-behaved electrostatic potential based method using charge restraints for deriving atomic charges: the RESP model. J Phys Chem 97:10269–10280. doi:10.1021/j100142a004
19. Zavodnik V, Stash A, Tsirelson V, De Vires R, Feil D (1999) Electron density study of urea using TDS-corrected X-ray diffraction data: quantitative comparison of experimental and theoretical results. Acta Cryst B55:45–54. doi:10.1107/S0108768198005746
20. Vaughan P, Donohue J (1952) The structure of urea. Interatomic distances and resonance in urea and related compounds. Acta Cryst 5:530–535. doi:10.1107/S0365110X52001477
21. Worsham JE, Levy HA, Peterson SE (1957) The positions of hydrogen atoms in urea by neutron diffraction. Acta Cryst 10:319–323. doi:10.1107/S0365110X57000924
22. Materials Studio 5.0 (2009), Accelrys Software Inc., San Diego, CA.
23. Case DA, Darden TA, Cheatham TE III, Simmerling CL, Wang J, Duke RE, Luo R, Crowley M, Walker RC, Zhang W, Merz KM, Wang B, Hayik S, Roitberg A, Seabra G, Kolossváry I, Wong KF, Paesani F, Vanicek J, Wu X, Brozell SR, Steinbrecher T, Gohlke H, Yang L, Tan C, Mongan J, Hornak V, Cui G, Mathews DH, Seetin MG, Sagui C, Babin V, Kollman PA (2008) AMBER 10. University of California, San Francisco
24. Essmann U, Perera L, Berkowitz ML, Darden T, Lee H, Pedersen LG (1995)A smooth particle mesh Ewald method. J Chem Phys 103:8577-8593. doi:10.1063/1.470117
25. Darden T, York D, Pedersen L (1993) Particle mesh Ewald: An N log(N) method for Ewald sums in large systems. J Chem Phys 98:10089–10092. doi:10.1063/1.464397
26. Civalleri B, Doll K, Zicovich-Wilson CM (2007) *Ab initio* investigation of structure and cohesive energy of crystalline urea. J Phys Chem B 111:26–33. doi:10.1021/jp065757c
27. Civalleri B, Zicovich-Wilson CM, Valenzano L, Ugliengo P (2008) B3LYP augmented with an empirical dispersion term (B3LYP-D*) as applied to molecular crystals. Cryst Eng Comm 10:405–410. doi:10.1039/B715018K
28. Case DA, Darden TA, Cheatham TE III, Simmerling CL, Wang J, Duke RE, Luo R, Merz KM, Pearlman DA, Crowley M, Walker RC, Zhang W, Wang B, Hayik S, Roitberg A, Seabra G, Wong KF, Paesani F, Wu X, Brozell S, Tsui V, Gohlke H, Yang L, Tan C, Mongan J, Hornak V, Cui G, Beroza P, Mathews DH, Schafmeister C, Ross WS, Kollman PA (2006) AMBER 9. University of California, San Francisco
29. Turzi SS (2011) On the Cartesian definition of orientational order parameters. J Math Phys 52:053517
30. Suzuki K, Onishi S, Koide T, Seki S (1956) Vapor pressures of molecular crystals. XI Vapor pressures of crystalline urea and diformylhydrazine. Energies of hydrogen bonds in these crystals. Bull Chem Soc Jpn 29:127–131. doi:10.1246/bcsj.29.127
31. Ferro D, Barone G, Della Gatta G, Piacente V (1978) Vapour pressures and sublimation enthalpies of urea and some of its derivatives. J Chem Thermodyn 9:915–923. doi:10.1016/0021-9614(87)90038-3
32. Emel'yanenko VN (2006) Measurement and prediction of thermochemical properties: improved increments for the estimation of enthalpies of sublimation and standard enthalpies of formation of alkyl derivatives of urea. J Chem Eng Data 51:79–87. doi:10.1021/je050230z
33. Zaitsau DZ, Kabo GJ, Kozyro AA, Sevruk VM (2003) The effect of the failure of isotropy of a gas in an effusion cell on the vapor pressure and enthalpy of sublimation for alkyl derivatives of carbamide. Thermochimica Acta 406:17–28. doi:10.1016/S0040-6031(03)00231-4
34. De Wit HGM, van Miltenburg JC, De Kruif CG (1983) Thermodynamic properties of molecular organic crystals containing nitrogen, oxygen, and sulphur 1. Vapour pressures and enthalpies of sublimation. J Chem Thermodyn 15:651–663. doi:10.1016/002-9614(83)90079-4
35. Gora RW, Bartkowiak W, Roszak S, Leszczynski J (2002) A new theoretical insight into the nature of intermolecular interactions in the molecular crystal of urea. J Chem Phys 117:1031–1039. doi:10.1063/1.1482069
36. Tsuziki S, Orita H, Honda K, Mikami M (2010) First-principles lattice energy calculation of urea and hexamine crystals by a combination of periodic DFT and MP2 two-body interaction energy calculations. J Phys Chem B 114:6799–6805. doi:10.1021/jp912028q
37. Brunsteiner M, Price SL (2001) Morphologies of organic crystals: sensitivity of attachment energy predictions to the model intermolecular potential. Cryst Growth Des 1:447–453. doi:10.1021/cg015541u
38. Boek ES, Feil D, Briels WJ, Bennema P (1991) From wave function to crystal morphology: Application to urea and alpha-glycine. J Cryst Growth 114:389–410. doi:10.1016/0022-0248(91)90057-C
39. Kabo G Ya, Miroshnichenko EA, Frenkel ML, Kozyro AA, Simirskii VV, Krasulin AP, Vorob'eva VP, Lebedev Yu A (1990) Thermochemistry of urea alkyl derivatives. Bull Acad Sci USSR, Div Chem Sci 662-667
40. Stephenson RM, Malanowski S (1987) Handbook of the thermodynamics of organic compounds. Elsevier, New York
41. Trimble LE, Voorhoeve RJH (1978) Continuous colorimetric monitoring of vapour-phase urea and cyanates. Analyst 103:759–765. doi:10.1039/AN9780300759
42. Bradley RS, Cleasby TG (1953) The vapour pressure and lattice energy of hydrogen-bonded crystals. Part I. Oxamide, oxamic acid, and rubeanie acid. J Chem Soc London 1681-16.
43. Paorici C, Zha M, Zanotti L, Attolini G, Traldi P, Catinella S (1995) Thermodynamic analysis of urea physical vapour transport. Cryst Res Technol 30:667–675. doi:10.1002/crat.2170300513
44. Aylward GH, Findlay TJV (1986) Datensammlung Chemie in SI Einheiten, 2nd edn. Chemie, Weinheim

45. Tartaglino U, Zykova-Timan T, Ercolessi F, Tosatti E (2005) Melting and nonmelting of solid surfaces and nanosystems. Phys Reports 411:291–321. doi:10.1016/j.physrep.2005.01.004
46. Weiner SJ, Kollman PA, Case DA, Singh UC, Ghio C, Alagona G, Profeta S, Weiner P (1984) A new force field for molecular mechanical simulation of nucleic acids and proteins. J Am Chem Soc 106:765–784. doi:10.1021/ja00315a051
47. Haleblian J, McCrone W (1969) Pharmaceutical applications of polymorphism. J Pharm Sci 58:911–929. doi:10.1002/jps.2600580802
48. Coombes DS, Catlow CRA, Gale JD, Hardy MJ, Saunders MR (2002) Theoretical and experimental investigations on the morphology of pharmaceutical crystals. J Pharm Sci 91:1652–1658. doi:10.1002/jps.10148
49. Anwar J, Zahn D (2011) Uncovering molecular processes in crystal nucleation and growth by using molecular simulation. Angewandte Chem Int Edn 50:1996–2013. doi:10.1002/anie.201000463
50. Kawska A, Brickmann J, Hochrein O, Zahn D (2005) From amorphous aggregates to crystallites: modelling studies of crystal growth in vacuum. Z Anorg Allg Chem 631:1172–1176. doi:10.1002/zaac.200400548
51. Kawska A, Brickmann J, Kniep R, Hochrein O, Zahn D (2006) An atomistic simulation scheme for modeling crystal formation from solution. J Chem Phys 124:024513-1-024513-7. doi:10.1063/1.2145677
52. Kawska A, Duchstein P, Hochrein O, Zahn D (2008) Atomistic mechanisms of ZnO aggregation from ethanolic solution: ion association. Proton Transfer, and Self-Organization Nano Lett 8:2336–2340. doi:10.1021/nl801169x